Slow rotational mobilities of antibodies and lipids associated with substrate-supported phospholipid monolayers as measured by polarized fluorescence photobleaching recovery

Melanie M. Timbs and Nancy L. Thompson
Department of Chemistry, University of North Carolina at Chapel Hill, Chapel Hill, North Carolina 27599-3290 USA

ABSTRACT Polarized fluorescence photobleaching recovery has been used to monitor slow rotational motions of a fluorescently-labeled anti-dinitrophenyl mouse IgG1 monoclonal antibody (ANO2) specifically bound to substrate-supported monolayers composed of a mixture of distearoylphosphatidylcholine (DSPC) and dinitrophenyldioleoylphosphatidylethanolamine (DNP-DOPE). ANO2 antibodies were labeled with a new bifunctional carbocyanine fluorophore that has two amino-reactive groups; steady-state fluorescence anisotropy data confirmed the expected result that the ANO2-conjugated bifunctional probe had less independent flexibility than ANO2-conjugated unifunctional fluorescence labels. Rotational mobilities were also measured for the fluorescent lipid 1,1'-dioctadecyl 3,3,3',3'-tetramethylindocarbocyanine (dil) in DSPC and in mixed DSPC/DNP-DOPE monolayers in the presence and absence of unlabeled ANO2 antibodies.

The apparent rotational correlation time and fractional mobility of ANO2 on supported monolayers were ~70 and ~0.3 s, respectively. These measured parameters of rotational mobility did not depend on the ANO2 surface density or on kinetic factors, but addition of unlabeled polyclonal anti-(mouse IgG) antibodies significantly decreased the apparent mobile fraction. The measured fluorescence recovery curves for dil were consistent with two fluorophore populations with rotational correlation times of ~4 and ~100 s and a population of immobile fluorescent lipid. No difference in fluorescence recovery and decay curves was measured for dil in DSPC monolayers, DSPC/DNP-DOPE monolayers, and DSPC/DNP-DOPE monolayers treated with unlabeled ANO2 antibodies.

INTRODUCTION

A phagocytotic cell such as a macrophage specifically recognizes, engulfs, and digests antibody-coated foreign matter. Of interest are the molecular events in the region of membrane–membrane contact that govern the antibody-mediated phagocytotic process. In particular, understanding correlations between antibody dynamics and activation of the phagocytotic response may provide insight into the mechanics of signal generation and signal transduction across the phagocytotic cell membrane, may aid in the elucidation of the requirements for an optimal phagocytotic response and may provide analogies for other receptor-mediated processes. One method of investigating molecular motion and interaction in the macrophage-target contact region is to replace the target cell membrane with a substrate-supported planar model membrane and to employ techniques in fluorescence microscopy. Fluorescence techniques provide a sensitive method of monitoring the organization and dynamics of film-bound antibodies and thus of characterizing the requirements for and effects of macrophage response to antibody-coated model membranes.

Supported planar model membranes have been used to study a variety of membrane processes (McConnell et al., 1986; Thompson and Palmer, 1988; Thompson et al., 1988). In particular, antibodies specifically recognize and bind to phospholipid Langmuir-Blodgett films containing hapten-conjugated phospholipids. The bound antibodies can be translationally mobile or immobile or arranged in ordered arrays called two-dimensional crystals (Subramaniam et al., 1986; Tamm, 1988; Wright et al., 1988; Uzgiris and Kornberg, 1983; Uzgiris, 1986). The translational diffusion (mobile antibodies) and crystal structures (immobile antibodies) are sensitive functions of the physical and chemical properties of the films, of the structure and density of bound antibodies and of the solution properties. In addition, macrophages and macrophage-related cell lines specifically bind and metabolically respond to Langmuir-Blodgett films containing bound antibodies (Hafeman et al., 1981; Kimura et al., 1986).

This paper describes the use of polarized fluorescence photobleaching recovery (PFPR; Smith et al., 1981; Velez and Axelrod, 1988; Scalettar et al., 1988, 1990) to monitor slow rotational motions of anti–dinitrophenyl monoclonal antibodies fluorescently labeled with a new bifunctional carbocyanine derivative and specifically bound to substrate-supported phospholipid monolayers containing a dinitrophenylated phospholipid. Rotational motions of a fluorescent lipid in the supported phospholipid monolayers were also measured. The results show that monolayer-bound antibodies have approximately the same rotational correlation time as the fluorescent lipids and that the antibody rotational correlation times do not

dramatically depend on the antibody surface density or on kinetic factors. Analysis of the PFPR data employs experimental measurements of the orientation distribution of fluorophore absorption dipoles made with polarized evanescent illumination (Thompson et al., 1984) and a generalization of the theoretical basis of PFPR (Velez and Axelrod, 1988) that includes multiple fluorophore populations.

THEORETICAL BACKGROUND

Rotational mobilities

In PFPR, fluorescent molecules are photochemically bleached with a pulse of linearly polarized light. The fluorescence intensities monitored with linearly-polarized light oriented parallel, $F_\parallel(t)$, or perpendicular, $F_\perp(t)$, to the bleach polarization increase and decrease, respectively, with time. The rate and shape of the fluorescence recovery and decay provide information about the rotational mobility of the fluorescent molecules relative to the direction of light propagation. A theoretical basis for PFPR has been developed by a number of groups (Smith et al., 1981; Wegener, 1984; Wegener and Rigler, 1984; Dale, 1985, 1987; Velez and Axelrod, 1988).

The relationship between the postbleach fluorescence intensities $F_{\parallel,\perp}(t)$ and the prebleach fluorescence intensity $F(-)$ is described by the normalized postbleach change in fluorescence intensities

$$\Delta F_{\parallel,\perp}(t) = [F(-) - F_{\parallel,\perp}(t)]/F(-). \quad (1)$$

For azimuthally-symmetric, two-dimensional samples in which all fluorophores are equivalently oriented and fully rotationally mobile about the normal to the sample during the observed time,

$$\Delta F_{\parallel,\perp}(t) = a \pm be^{-4Dt} - ce^{-16Dt}, \quad (2)$$

where a, b, and c are positive constants that depend in a known manner on the bleaching depth and on the orientation and flexibility of the absorption and emission dipoles and D is the rotational diffusion coefficient (Velez and Axelrod, 1988). For all but very deep bleaching, the constant c is small and is therefore assumed equal to zero. The normalized fluorescence recoveries and decays, $\Delta F_\parallel(t)$ and $\Delta F_\perp(t)$, thus contain three independent and measurable constants (a, b, and D).

The anisotropy $r(t)$, defined as

$$r(t) = \frac{[\Delta F_\parallel(t) - \Delta F_\perp(t)]}{[\Delta F_\parallel(t) + 2\Delta F_\perp(t)]}, \quad (3)$$

is less sensitive to postbleach fluorescence changes that do not arise from rotational mobility than the functions $\Delta F_\parallel(t)$ and $\Delta F_\perp(t)$. Using Eq. 2 with $c = 0$ in Eq. 3 yields

$$r(t) = \frac{2(b/a)e^{-4Dt}}{3 - (b/a)e^{-4Dt}}. \quad (4)$$

A convenient method of measuring the values of a, b, and D is to obtain D and the ratio b/a from the anisotropy $r(t)$ and constant a from the average fractional bleach:

$$a = \tfrac{1}{2}[\Delta F_\parallel(0) + \Delta F_\perp(0)]. \quad (5)$$

The relationship of constants a, b, and D to $F_{\parallel,\perp}(t)$ and $r(t)$ are illustrated in Fig. 1. At long times, $F_\parallel(\infty) = F_\perp(\infty)$ and $r(\infty) = 0$.

For two-dimensional samples in which different populations of fluorophores rotationally diffuse with coefficients D_i and in which all populations are bleached with equal efficiency, a straightforward generalization of Eqs. 1–5 shows that, for R fluorophore types of relative abundance f_i,

$$\Delta F_{\parallel,\perp}(t) = \sum_{i=1}^{R} f_i[a_i \pm b_i e^{-4D_i t} - c_i e^{-16D_i t}], \quad (6)$$

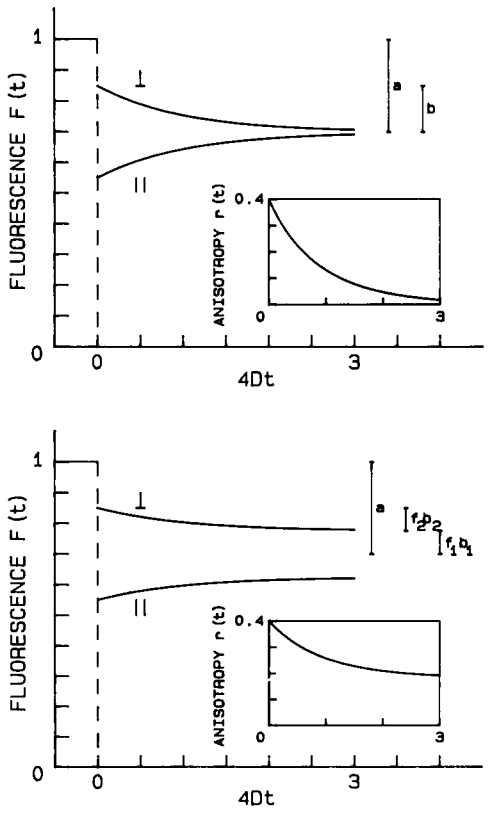

FIGURE 1 Theoretical shape of fluorescence recovery $F_\parallel(t)$, decay $F_\perp(t)$, and anisotropy $r(t)$ for PFPR. Curves are calculated using (*top*) Eqs. 1, 2, and 4 with $a = 0.3$, $b = 0.15$, $c = 0$, and $F(-) = 1$; and (*bottom*) Eqs. 1, 2, and 7 with $a = 0.3$, $R = 2$, $f_1b_1 = f_2b_2 = 0.075$, $c = 0$, $D_1 = 0$, $D_2 = D$, and $F(-) = 1$.

where a_i and b_i depend on the orientation distribution of the i th population and the bleaching depth and $c_i \approx 0$. Eqs. 3 and 6 imply that

$$r(t) = \frac{2\sum_{i=1}^{R}(f_i b_i/a)e^{-4D_i t}}{3 - \sum_{i=1}^{R}(f_i b_i/a)e^{-4D_i t}}, \quad (7)$$

where

$$a = \sum_{i=1}^{R} f_i a_i \quad (8)$$

equals the fractional bleach as defined in Eq. 5. Data for a sample with two fluorophore populations contain five independent and measurable parameters (a, f_1b_1, f_2b_2, D_1 and D_2) provided the time decays due to D_2 and D_1 can be resolved and are in the time range of measurement and data for a sample with three populations contain seven independent parameters. The constants f_i and b_i appear as a product and cannot be independently measured. However, if all populations have identical or similar values of $b_i = b$, then the fractional abundance of the ith population can be estimated from the measured values of f_ib_i as

$$f_i \approx f_i b_i \Big/ \left[\sum_{i=1}^{R} f_i b_i\right]. \quad (9)$$

Fig. 1 illustrates how $F_\parallel(t)$, $F_\perp(t)$, and $r(t)$ depend on a, f_1b_1, f_2b_2, and D_2 for a sample with both mobile ($D_2 = D$) and immobile ($D_1 = 0$) fluorophore populations. At long times, $F_\parallel(\infty) \neq F_\perp(\infty)$ and $r(\infty) \neq 0$.

As shown by Velez and Axelrod (1988), a and b are functions of the following variables: a constant proportional to the bleaching intensity, bleaching duration, and molar absorptivity that describes the depth of bleaching (B); the average tilt angle of absorption dipoles from the plane of the sample (ϵ); the semiangle of a cone in which the absorption dipoles wobble on a time scale faster than that of fluorescence bleaching (β); and the angle between the fluorophore absorption and emission dipole moments (χ). For dil in model membranes, both ϵ and χ are between 0 and 30° (Badley et al., 1973; Yguerabide and Stryer, 1971; Axelrod, 1979). For weak to moderate levels of bleaching ($B < 2$), low to moderate wobbling amplitudes ($\beta < 60°$), and $\epsilon = \chi = 0°$, constant a ranges from 0 to 0.6 and constant b ranges from 0 to 0.3 (Fig. 2 *A*). Given a wobble angle β and a bleach depth B, the values of the fractional bleach a and recovery b are slightly lower for $\epsilon = \chi = 30°$ than for $\epsilon = \chi = 0°$ (Fig. 2 *B*). Fig. 2 *C* depicts the $B - \beta$ curves for a two-dimensional sample of randomly-oriented fluorophores. For known values of ϵ and χ and measured values of a and b, the intersection of the lines of constant a and b in the $B - \beta$ plane determines the values of B and β. If more than one fluorophore population is present, then the values of a_i and b_i depend on B, χ, and the parameters of the orientation distribution of the ith population ϵ_i and β_i.

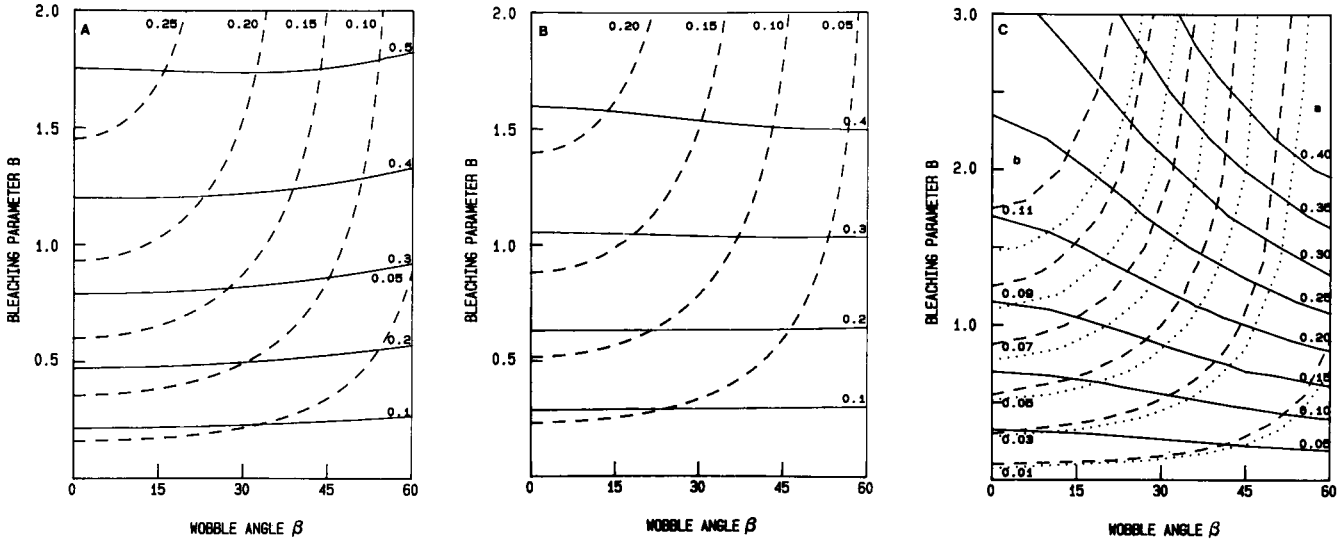

FIGURE 2 Theoretical values of constants a and b. These curves show the values of a (——) and b (---, · · ·) as a function of the bleaching parameter B and the wobble angle β. The tilt angle ϵ and the angle between the absorption and emission dipoles χ equal (*A*) 0° and (*B*) 30°. In *C*, angle ϵ is randomly distributed and angle χ equals 0° (---) or 30° (· · ·). Plots *A* and *B* were generated according to Eqs. 21 and 22 of Velez and Axelrod (1988) with $\psi_1 = 0$ and $\psi_2 = \beta$; plot *C* was obtained by numerical integration of Eqs. 21 and 22 over all ϵ.

Absorption dipole orientation distributions

The orientation distribution of absorption dipoles depends on angles ϵ and β and can be independently characterized by fluorescence microscopy as described previously (Thompson et al., 1984). In this technique, the fluorescence is measured as a function of the polarization of the exciting light with a high-aperture objective that collects nearly one-half of the emitted light. If the exciting light propagates normal to the membrane (e.g., with epi-illumination) then, in principle, information about azimuthally asymmetric distributions can be obtained. However, measurements over large areas of supported phospholipid monolayers should be exactly or approximately azimuthally symmetric. If the exciting light is the evanescent field produced by a light beam that is totally internally reflected at the substrate/solution interface, then rotating the polarization of the incident beam rotates the polarization of the evanescent field primarily between directions perpendicular and parallel to the interface and information about the tilt angle ϵ and the fast wobble angle β is obtained.

For azimuthally symmetric samples, the fluorescence excited with evanescent illumination and normalized to a maximum value of one is given by (Thompson et al., 1984)

$$I(\psi) = 1 + C(\cos^2\psi - \cos^2\psi_0), \tag{10}$$

where ψ is the angle that the beam polarization makes with the incidence plane, ψ_0 is the angle at which $I(\psi)$ is a maximum (0 or 90°), and C is a measured constant (positive or negative, respectively). The constant C depends on the following parameters: (*i*) the polarization of the evanescent field for different incident beam polarizations, which depends on the angle of incidence of the totally internally reflected beam (α) and the relative refractive index of the solution/glass interface (n), (*ii*) a constant that describes the relative fluorescence collection efficiency for emission dipoles oriented perpendicular or parallel to the optical axis of the objective ($1 - \gamma$), and (*iii*) the orientation distribution of fluorophore absorption dipoles. If the orientation distribution of absorption dipoles $N(\theta)$ is written as an expansion in Legendre polynomials $P_i(\cos\theta)$ with order parameters s_i, so that

$$N(\theta) = \sum_{i=1}^{\infty} s_i P_i(\cos\theta) \tag{11}$$

$$\int_{\text{all space}} N(\theta)\sin\theta\, d\theta = 1, \tag{12}$$

then C depends only on the order parameters s_2 and s_4 where $-1/2 \le s_2 \le 1$ and $-(3/7) \le s_4 \le 1$.

When the fluorescence collection parameter γ equals 0, the measured constant C depends only on s_2 and not on s_4 (Thompson et al., 1984). As shown in Fig. 3 *A*, the dependence of C on s_2 is strong and does not change significantly within the possible range of values for the incidence angle α ($64° = \sin^{-1}n \le \alpha \le 90°$) or the relative refractive index n (≈ 0.9). Thus, fairly accurate determination of s_2 is possible in the simplest case where

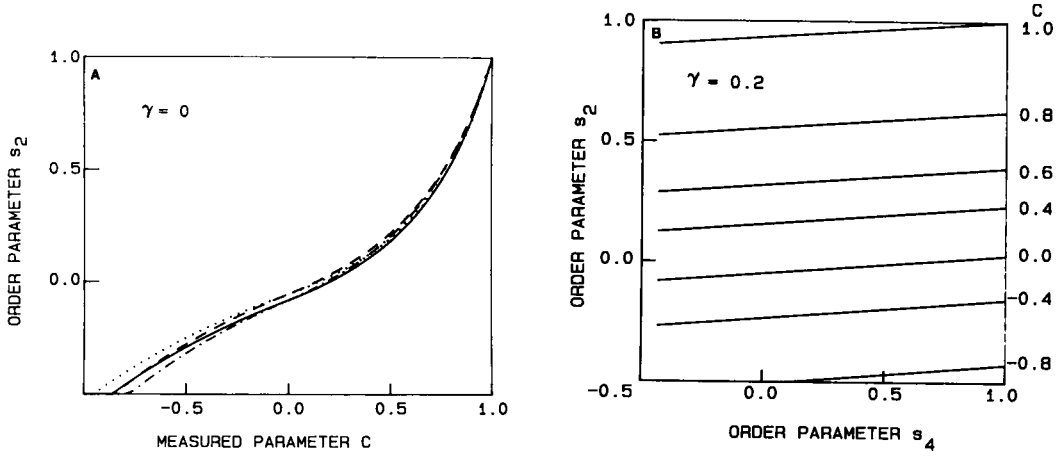

FIGURE 3 Fluorescence-detected absorption dichroism constant C. (*A*) When the fluorescence collection parameter γ equals 0, constant C is a monotonic function of s_2 and depends only weakly on the relative refractive index n and the incidence angle α; curves are for $\alpha = 70°$, $n = 0.88$ (——); $\alpha = 70°$, $n = 0.92$ (· · ·); $\alpha = 85°$, $n = 0.88$ (–·–); and $\alpha = 85°$, $n = 0.92$ (---). (*B*) When the fluorescence collection parameter γ equals 0.2, constant C depends only weakly on s_4; the plot is for $\alpha = 70°$ and $n = 0.89$. Plots were generated according to Eqs. 18 and 19 of Thompson et al. (1984).

$\gamma = 0$. In practice, however, the parameter $\gamma \neq 0$ because fluorescence is not collected over a full 2π steradians and because the substrate affects the angular distribution of fluorescence emitted from fluorophores with different orientations; previous work has shown that the value of γ for the conditions used in this study is ≈ 0.1 (Burghardt and Thompson, 1984). Nonzero γ introduce s_4 dependence in C, but as shown in Fig. 3 *B* the dependence is weak for small γ ($= 0.2$), and the s_2 value that corresponds to a given measured value of C is approximately equal to the value that would be obtained from Fig. 3 *A* when $\gamma = 0$.

For stationary dipoles uniformly oriented at a single polar angle $90° - \epsilon$, Eqs. 11 and 12 imply that

$$s_2 = (1/2)(3 \sin^2 \epsilon - 1), \tag{13}$$

and a given measured value of s_2 specifies the tilt angle ϵ. A more general treatment is required if the absorption dipoles rapidly fluctuate about their average orientation within a characteristic angle β (Badley et al., 1973). As shown in Appendix A for a model in which dipoles are found within a cone of semiangle β centered at tilt angle ϵ, the relationship between s_2, ϵ, and β is given by

$$s_2 = (1/4)(3 \sin^2 \epsilon - 1) \cos\beta\,(1 + \cos\beta). \tag{14}$$

In this case, a given measured value of s_2 is consistent with a range of pairs of ϵ and β. Other models for the functional form of the orientation distribution of absorption dipoles may also be appropriate, but this model has been chosen for consistency with the theoretical treatment of PFPR developed by Velez and Axelrod (1988).

Steady-state anisotropies of fluorescent probes on antibodies in solution

Information about rapid motions of fluorophores conjugated to antibodies can be obtained by measuring steady-state anisotropies in solution. A simple expression for the anisotropy A of a spherical fluorophore that is attached to a spherical macromolecule and experiences rotational motion independent of the macromolecular motion is (Leach, 1969)

$$A(T/\eta) = \frac{A_0(1 - q)}{1 + (C_p T/\eta)} + \frac{A_0 q}{1 + (C_p T/\eta) + (C_f T/\eta)}, \tag{15}$$

where A_0 is the limiting anisotropy, q is a constant related to the amount of independent fluorophore motion, T is the absolute temperature, η is the viscosity,

$$C_p = \frac{k\tau}{6V_p}, \qquad C_f = \frac{k\tau}{6V_f}, \tag{16}$$

k is Boltzmann's constant, τ is the fluorescence lifetime, V_p is the hydrodynamic volume of an antibody, and V_f is the molecular volume that corresponds to the correlation time of independent fluorophore rotational flexibility. Although a number of possible phenomena such as antibody segmental flexibility and the nonspherical shape of both the antibody and probe are not included in Eq. 15, the values of C_f/C_p and q provide an indication of the degree of independent fluorophore rotational mobility.

MATERIALS AND METHODS

Antibodies

Mouse and sheep polyclonal IgG (Sigma Chemical Co., St. Louis, MO) and goat anti-(mouse IgG) (Jackson ImmunoResearch Labs, West Grove, PA) were dialyzed against phosphate-buffered saline (PBS, 0.05 M sodium phosphate, 0.15 M sodium chloride, 0.01% sodium azide, pH 7.4) and passed through a 0.22-μm filter. The mouse IgG1 anti-dinitrophenyl monoclonal antibody ANO2 (Balakrishnan et al., 1982) was purified from cell culture supernatants by protein A affinity chromatography (Anglister et al., 1984; Wright et al., 1988), dialyzed against PBS, and stored at −15°C.

ANO2 antibodies were labeled with the new bifunctional, amine-reactive, tetramethylindocarbocyanine fluorophore CY3.18 (a generous gift of Alan Waggoner and Ratan Majumdar of Carnegie Mellon University; Wagner et al., 1990; C-ANO2) by treating 0.1–0.3 mg/ml ANO2 in 0.1 M $NaHCO_3/Na_2CO_3$ pH 9.5 with a 12-fold molar excess of dye in 10–20 μl anhydrous dimethylformamide for 1 h at room temperature. ANO2 antibodies were labeled with fluorescein isothiocyanate (Molecular Probes, Inc., Eugene, OR; F-ANO2) and tetramethylrhodamine isothiocyanate (Molecular Probes, Inc.; R-ANO2) according to published procedures (Mishell and Shiigi, 1980). Fluorescently-labeled ANO2 was purified by Sephadex G50-80 chromatography in PBS, dialysis against PBS, 0.22 μm filtration, and sedimentation at 100,000 *g* for 1–2 h. Labeled antibodies were stored at 4°C and used within 3 wk.

ANO2 concentrations and the molar ratios of fluorophore to ANO2 (F:A) were determined spectrophotometrically using the following estimated absorptivities and measured ratios of fluorophore absorptivities at 280 nm to those at their absorption maxima:[1] ANO2, 210,000 $M^{-1}\,cm^{-1}$ (280 nm); carbocyanine fluorophore, 130,000 $M^{-1}\,cm^{-1}$ (550 nm), 0.13 (280 nm/550 nm); fluorescein, 75,000 $M^{-1}cm^{-1}$ (494 nm), 0.25 (280 nm/494 nm); tetramethylrhodamine, 75,000 $M^{-1}cm^{-1}$ (550 nm), 0.36 (280 nm/550 nm). The spectrophotometrically-determined fluorophore-to-antibody ratios ranged from one to three except as noted. Sodium dodecyl sulfate polyacrylamide gel electrophoresis (SDS-PAGE) of labeled and unlabeled ANO2 was carried out according to standard procedures. In some experiments (as noted), 0.1 ml of 0.1 mg/ml ANO2 in PBS was first treated with a 100- to 800-fold molar excess of disuccinimidylsuberate (Pierce Chemical Co., Rockford, IL) in 10 μl dimethylsulfoxide.

[1]Labeled ANO2 concentrations were also determined by the method of Lowry et al. (Peterson, 1979) using unlabeled ANO2 as a standard. These concentrations were 10–30% higher than the spectrophotometrically-determined concentrations, and the discrepancy could not be accounted for by chemical effects of fluorophores on the Lowry assay or by uncertainties in the fluorophore absorptivities. Concentrations are given as spectrophotometric estimates throughout.

The specificity of unlabeled ANO2 and C-ANO2 for dinitrophenyl (DNP) was confirmed by monitoring the quenching of the fluorescence (SLM 8000C, Inc., Urbana, IL) of ANO2 in PBS (10–30 μg/ml) by DNP-glycine (Sigma Chemical Co.) with excitation and emission wavelengths equal to 280 and 334 nm, respectively. The independent rotational mobility of ANO2-conjugated fluorophores was examined by measuring the steady-state fluorescence anisotropies as a function of viscosity in PBS/glycerol (10–50 μg/ml) with excitation and emission wavelengths as follows: R-ANO2 and C-ANO2, 550 and 565 nm; F-ANO2, 494 and 520 nm.

Supported phospholipid monolayers

All water was purified to exceed standards for type I reagent grade water. Distearoylphosphatidylcholine (DSPC; Sigma Chemical Co.), dinitrophenyldioleoylphosphatidylethanolamine (DNP-DOPE; Avanti Polar Lipids, Birmingham, AL) and 1,1'-dioctadecyl-3,3,3',3'-tetramethylindocarbocyanine perchlorate (diI; Molecular Probes, Inc., Eugene, OR) were judged to be pure by thin layer chromatography. Monolayers of DSPC, DSPC:diI (99.5:0.5, mol/mol), DSPC:DNP-DOPE:diI (70:29.5:0.5, mol/mol/mol) or DSPC:DNP-DOPE (70:30, mol/mol) were spread from hexane:ethanol (9:1) at 100 Å^2/molecule on the air/water interface of a Joyce-Loebl Langmuir Trough (model 4, Vickers Instruments, Inc., Malden, MA) at room temperature (24–28°C). The monolayers were compressed at 1–2 Å^2/molecule per min to a final surface pressure of 35 dyn/cm. Single phospholipid monolayers were deposited on glass microscope slides treated with octadecyltrichlorosilane (Aldrich Chemical Co., Milwaukee, IL) by vertical dipping at 5.4 mm/min (von Tscharner and McConnell, 1981; Thompson et al., 1984; Wright et al., 1988).

For measurements in the absence of antibodies, substrate-supported monolayers were transferred to a sample chamber in PBS. For measurements in the presence of antibodies, monolayers were washed with 1 ml PBS, treated with sheep IgG in PBS (200 μl, 0.1 mg/ml) for 2 min, treated with one of the following procedures, and then washed with 3 ml PBS: (*i*) ANO2 or C-ANO2 (200 μl, 20 μg/ml, and 10 min unless otherwise indicated); (*ii*) ANO2 (100 μl, 0.86 mg/ml, 5 min) followed by a mixture of C-ANO2 (20 μg/ml) and ANO2 (0.64 mg/ml) (200 μl, 10 min); or (*iii*) a mixture of C-ANO2 (20 μg/ml) and DNP-glycine (1.3 mM) (200 μl, 10 min). Some samples were further treated with unlabeled, polyclonal anti-(mouse IgG) (200 μl, 0.1 mg/ml, 10 min) and washed with 1 ml PBS. All samples were transferred in PBS to a sample holder suitable for microscopy and brought to 18°C with a thermoelectrically-cooled microscope stage (Wright et al., 1988).

Polarized fluorescence photobleaching recovery

The fluorescence microscope was constructed from an inverted optical microscope (Zeiss IM-35), the 514.5-nm line of an argon ion laser (Coherent Innova 90-3), a single-photon counting photomultiplier (RCA 31034A), and an IBM PC AT microcomputer, as previously described (Fig. 4; Palmer and Thompson, 1989; Poglitsch and Thompson, 1989). The apparatus was configured to measure rotational mobilities according to previous designs (Smith et al., 1981; Velez and Axelrod, 1988). The laser beam was split into bleaching and observation beams; the bleaching beam passed through a polarization rotator (Lexel Corp., Palo Alto, CA). Both beams were passed through a beam expander (Edmund Scientific Co., Barrington, NJ), reflected by a dichroic mirror and focused through an objective (Nikon, 40×, 0.55 NA, air) to illuminate a Gaussian-shaped area of radius ~25 μm (diI) or ~38 μm (C-ANO2). Fluorescence was collected through a linear polarizer aligned with the observation beam polarization and an image

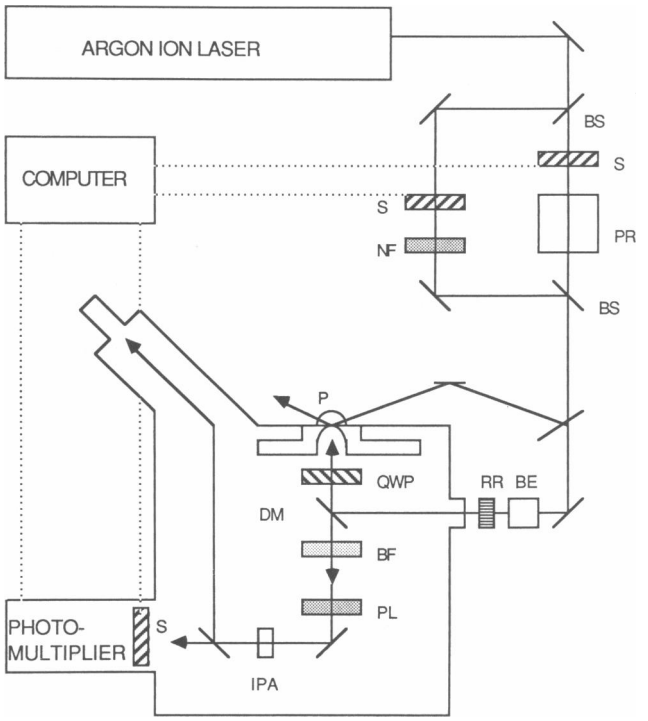

FIGURE 4 Optical apparatus. Fluorescence microscope: /, mirror; *BS*, 90%/10% beam splitter; *S*, computer-controlled mechanical shutter; *NF*, neutral density filter; *PR*, polarization rotator; *P*, hemicylindrical fused silica prism; *BE*, beam expander; *RR*, Rhonchi ruling; *QWP*, quarter wave plate; *DM*, dichroic mirror; *BF*, barrier filter; *PL*, linear polarizer; *IPA*, image plane aperture.

plane aperture that restricted fluorescence collection to the illuminated area. The relative intensity of the bleaching beam when parallel or perpendicular to the monitoring beam was determined to equal 1.032 ± 0.004 by measuring the fluorescence of a solution of CY3.18 in PBS/ethanol (19:1) with the analyzing polarizer removed. The polarization of the exciting light in the sample plane was estimated by measuring the intensity of the laser beam passing through a polarizer placed above the objective and aligned parallel or perpendicular to the beam polarization with a photodiode; the average intensity ratio was 100 ± 15.

Fluorescence photobleaching parameters were as follows: observation and bleaching laser powers, 3–30 μW and ≤ 0.4 W, respectively; bleaching pulse duration, 50 ms (diI) to 2 s (C-ANO2); depth of bleaching, 15–35%. The temperature rise during the bleach pulse was estimated (Axelrod, 1977) to equal ~1°C assuming that the carbocyanine absorptivity and quantum efficiency were 130,000 $M^{-1}cm^{-1}$ and 0.5, respectively, and that the bleaching beam was attenuated in power by a factor of two by the optical elements between the laser aperture and the sample.

Fluorescence recovery curves were monitored for bleaching polarizations parallel and perpendicular to the observation polarization. The sets of curves $F_\parallel(t)$ and $F_\perp(t)$ for a given sample type and data set were normalized to prebleach fluorescence intensities of one and then averaged. The averages of $F_\parallel(t)$ and $F_\perp(t)$ were then used to calculate the fluorescence changes $\Delta F_\parallel(t)$ and $\Delta F_\perp(t)$ according to Eq. 1 and the anisotropy $r(t)$ and the value of constant a were calculated according to Eqs. 3 and 5. Values for the parameters $f_\parallel b_i/a$ and D_i were obtained from iterative Gauss-Newton fits of $r(t)$ to Eq. 7 with $D_\parallel = 0$.

Depolarized fluorescence photobleaching recovery

To assess the potential contribution of phenomena other than rotational mobility to the observed fluorescence recovery and decay under linearly polarized conditions, fluorescence recovery curves were obtained using circularly polarized bleaching and observation beams. The analyzing polarizer was removed and the laser beam was circularly polarized by a quarter wave plate (Dale, 1985; Melles-Griot, Irvine, CA) below the objective; the ratio of the laser intensities at the sample measured through a linear polarizer aligned parallel or perpendicular to the initial beam polarization was 0.96 ± 0.01. Apparent lateral diffusion coefficients were measured with fluorescence pattern photobleaching recovery (Smith and McConnell, 1978; Wright et al., 1988) with circularly polarized light and a spatial periodicity of 8 μm. Other experimental parameters were as listed above.

Fluorescence-detected absorption dichroism

To measure the absorption dichroism as a function of the polar angle from the substrate normal, the laser beam was passed through the polarization rotator and was totally internally reflected at the monolayer/solution interface through a hemicylindrical fused silica prism (Harrick Scientific Corp., Ossining, NY) at an incidence angle of α ~70°. Evanescently excited fluorescence was collected through a high-aperture microscope objective (Nikon, 60×, 1.4 N.A.), a 550-nm cutoff filter, and an image plane aperture that restricted fluorescence collection to the elliptically illuminated area (~30 × 100 μm). To measure the absorption dichroism as a function of the azimuthal angle about the substrate normal, the laser beam was passed through the polarization rotator and was then reflected by the dichroic mirror and focused on the sample through a microscope objective (Zeiss, 40×, 0.75 N.A.). Fluorescence was collected through the dichroic filter, a barrier filter, and the image plane aperture. To quantitatively analyze the experimentally obtained $I(\psi)$, the data were normalized so that $I(\psi)$ for a sample in which it was assumed that the fluorophore absorption dipoles were randomly oriented (C-ANO2 antibodies adsorbed to glass) had a value of C equal to the theoretical value for $\alpha = 70°$, $n = 0.89$, and $\gamma = 0.1$ ($C = 0.16$). The normalized curves $I(\psi)$ were fit to Eq. 10 with a Gauss-Newton routine to obtain values for C.

RESULTS

CY3.18-labeled ANO2 antibodies

ANO2 antibodies were labeled with the bifunctional fluorophore CY3.18 because a probe attached at two positions rather than one should experience less independent flexibility and therefore more accurately report the rotational motions of the antibody to which it is bound. Fluorescently-labeled (C-ANO2, R-ANO2, and F-ANO2) and unlabeled (ANO2) antibodies were analyzed with SDS-PAGE under reducing and nonreducing conditions and stained with Coomassie blue. All types of ANO2 antibodies ran as bands with appropriate apparent molecular weights. Observation of unstained gels under ultraviolet illumination indicated that both the heavy and light chains were fluorescently labeled for all three fluorophores and that no detectable unreacted fluorophore was present. Comparison of fluorescently-labeled ANO2 with ANO2 cross-linked by disuccinimidylsuberate on overloaded gels and stained with silver indicated that the bifunctional carbocyanine label but not fluorescein or tetramethylrhodamine isothiocyanate cross-linked a small fraction of the ANO2 polypeptides and that at least some of the cross-links were intermolecular. The quantity of CY3.18 -induced antibody aggregates was higher when the labeling reaction was carried out at higher ANO2 and fluorophore concentrations (F:A ≥ 5). The amount of cross-linked C-ANO2 that was present was judged to be insignificant for the preparations used in the experiments reported herein (1 ≤ F:A ≤ 3).

Quenching of ultraviolet-excited antibody fluorescence by DNP-glycine was significantly greater for ANO2 and C-ANO2 than for polyclonal mouse IgG. Solution association constants were obtained from these data using an iterative procedure that determines the free DNP-glycine concentration, corrects for collisional quenching using data for polyclonal mouse IgG, and finds the best fit to the functional form that describes a simple bimolecular reaction (Pisarchick, M. L., and N. L. Thompson, submitted for publication). The analysis yielded a DNP-glycine association constant of $1.8 \pm 0.5 \times 10^6\ M^{-1}$ for unlabeled ANO2, which equals one previously reported measurement (Anglister et al., 1984) and is within a factor of two of another reported measurement (Leahy et al., 1986). The measured equilibrium constant for C-ANO2 was $1.7 \pm 0.1 \times 10^6\ M^{-1}$, which is equivalent to the value for ANO2 and indicates that the presence of covalently-bound bifunctional carbocyanine fluorophore did not significantly alter ANO2 hapten recognition. Heavily-labeled C-ANO2 (F:A ≥ 5; not used in subsequent experiments) showed a slightly decreased affinity for DNP-glycine.

Mobility of ANO2-conjugated fluorescent probes

To examine the relative flexibility of antibody-bound fluorophores, steady-state anisotropies were measured as a function of viscosity. As shown in Fig. 5, the anisotropies of R-ANO2 and F-ANO2 were dependent on the viscosity, whereas the C-ANO2 anisotropy was not. The differences between the steady-state anisotropies for solutions of the lowest and highest viscosities were much larger for R-ANO2 (0.128 ± 0.005) and F-ANO2 (0.092 ± 0.013) than for C-ANO2 (0.009 ± 0.003) (Table 1).

The data in Fig. 5 were fit to the functional form of Eq. 15 with $1/A$ as the ordinate and T/η as the abscissa; T = 296°K; η ranging from 0.01 to 0.28 Poise; C_f and q as free

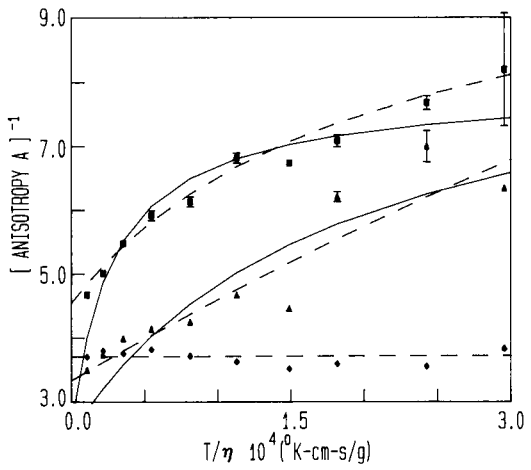

FIGURE 5 Steady-state anisotropy as a function of viscosity. Shown are the measured anisotropies for (♦) C-ANO2, (▲) R-ANO2, and (■) F-ANO2 and the best fits to Eq. 15 with $A_o = 0.4$ and with q and C_f as free parameters (—) and with A_o, q, and C_f as free parameters (---).

parameters; $V_p = 2.3 \times 10^{-19}$ cm^3/molecule; $\tau = 3.65$ ns (fluorescein), $\tau = 2.34$ ns (tetramethylrhodamine), or $\tau = 1$ ns (carbocyanine) (Chen and Scott, 1985; Packard and Wolf, 1985); and $A_o = 0.4$ (the theoretical maximum which corresponds to aligned absorption and emission dipoles moments). In this analysis, the ratio C_f/C_p and the parameter q were large for both F-ANO2 and R-ANO2, suggesting that fluorophore mobility contributed significantly to the observed anisotropies, but the viscosity-independent C-ANO2 data could not be well fit.

The data in Fig. 5 were also fit to Eq. 15 with A_o, C_f/C_p, and q as free parameters. The C-ANO2 data were best fit with $A_o = 0.27$ (corresponding to an interdipole angle of 28°) and either a small q or a small C_f/C_p ratio (e.g., $q = 0.05$; $C_f/C_p \leq 50$ or $q = 0.5$; $C_f/C_p \leq 10$). The values of q and C_f/C_p were still higher for F-ANO2 and R-ANO2 than the maximum estimated values for C-ANO2; the values of A_o (0.22–0.30) corresponded to absorption and emission dipole moments oriented at 24–33° (Table 1).

The data in Fig. 5 and Table 1 suggest that the bifunctional carbocyanine probe had less rotational mobility than the unifunctional probes. This lower apparent mobility of antibody-bound carbocyanine in the nanosecond time range means that, if all other factors are equivalent, this probe is a better choice for measurements of antibody rotational mobility. However, probe flexibility with any characteristic time that is faster than the bleaching duration will affect PFPR data and probe mobility with a characteristic time in the microsecond-millisecond time range would not be detected by measurements of the dependence of steady-state anisotropies on viscosity. The data also imply that ANO2-conjugated tetramethylrhodamine has less flexibility than fluorescein in the nanosecond-microsecond time range, suggesting increased noncovalent interactions between the tetramethylrhodamine probes and ANO2 antibodies to which they are attached.

Supported phospholipid monolayers

The fluorescence arising from dil in supported DSPC monolayers was nonuniformly distributed with optically resolved features of size 1–5 μm. The fluorescence of dil in DSPC/DNP-DOPE monolayers was also nonuniform, but the features were usually of a finer texture. The visual detection of spatially nonuniform dil fluorescence suggests the presence of coexistent solidlike and fluidlike domains similar to those previously observed in dipalmitoylphosphatidylcholine monolayers at the air/water

TABLE 1 Steady-state anisotropies for fluorophores conjugated to ANO2 antibodies

Fluorophore	Carbocyanine	Tetramethylrhodamine	Fluorescein
Anisotropies:			
A (PBS)	0.261 ± 0.002	0.158 ± 0.001	0.122 ± 0.013
A (PBS/glycerol)	0.270 ± 0.002	0.286 ± 0.005	0.214 ± 0.002
Two free parameters ($A_o = 0.4$)			
q	—	0.72	0.68
C_f/C_p	—	850	3100
Three free parameters			
A_o	0.27	0.30	0.22
q	0.05*	0.88	0.56
C_f/C_p	<50*	190	310

Steady-state anisotropies for ANO2-conjugated fluorophores in the least (PBS) and most (28% PBS/72% glycerol) viscous solutions are shown at the top. A_o, q, and C_f/C_p are from the best fits of the data in Fig. 5 to Eq. 15 with fixed parameters as described in the text. *C-ANO2 data were equally well fit with larger q values and smaller C_f/C_p ratios (e.g., $q = 0.5$ and $C_f/C_p < 10$).

interface (McConnell et al., 1984) and on alkylated substrates (Seul et al., 1985). The fluorescence measured over large areas (~2,000 μm^2) was uniform, with a typical standard deviation of 5–10% for 5–10 measurements on a single monolayer.

DSPC/DNP-DOPE supported monolayers containing bound C-ANO2 usually appeared uniformly fluorescent with a fine granular texture. However, distinct snowflake-shaped nonfluorescent regions of size 5–15 μm containing four to six main branches with multiple protrusions from each major branch were occasionally observed. These patterns, which may have been areas depleted of lipid, depleted of DNP-DOPE or containing sequestered DNP, were not readily reproducible. The presence of these nonfluorescent regions had no effect on the measured rotational mobility or the overall uniformity of the measured fluorescence over large areas. Typical standard deviations of 5–10 measurements of fluorescence intensity over large areas (~2,000 μm^2) were ~5% for DNP-DOPE/DSPC supported monolayers treated with C-ANO2.

Pretreatment of DNP-DOPE/DSPC monolayers with unlabeled ANO2 followed by addition of C-ANO2 and excess unlabeled ANO2 decreased the fluorescence intensity by ~98%. Addition of C-ANO2 combined with saturating amounts of DNP-glycine resulted in an ~90% decrease in fluorescence intensity. The ratio of the fluorescence of DNP-DOPE/DSPC monolayers treated with C-ANO2 to that of treated DSPC monolayers was as high as 200 (70 $\mu g/ml$). These results imply that C-ANO2 was specifically bound to DNP-DOPE in the supported monolayers.

As shown in Fig. 6, the measured fluorescence arising from C-ANO2 on DSPC/DNP-DOPE supported monolayers increased with the solution concentration of C-ANO2 with which monolayers were treated. The shape of the binding curve was qualitatively consistent with that previously measured for fluorescein-labeled ANO2 antibodies on supported bilayers composed of dimyristoylphosphatidylcholine and dinitrophenyl-conjugated dimyristoylphosphatidylethanolamine (Wright et al., 1988) and gave an apparent association constant of ~3 × 10^6 M^{-1}. C-ANO2 remained bound to DSPC/DNP-DOPE monolayers for at least 2 h.

Absorption dipole orientation distributions

The fluorescence $I(\psi)$ excited with epi-illumination over a 25-μm-radius circular area and as a function of the laser polarization ψ was equivalent within experimental error for dil in DSPC monolayers, dil in DSPC/DNP-DOPE monolayers untreated or treated with ANO2, C-ANO2 bound to DSPC/DNP-DOPE monolayers, and C-ANO2 nonspecifically adsorbed to glass substrates (data not shown). Thus, the orientation distributions of dil and CY3.18 absorption dipoles were azimuthally symmetric over large areas and Eq. 10 is applicable.

The fluorescence $I(\psi)$ excited with evanescent illumination was strongly dependent on ψ for dil in DSPC monolayers and in DSPC/DNP-DOPE monolayers untreated or treated with ANO2 (Fig. 7), whereas $I(\psi)$ was nearly independent of ψ for DSPC/DNP-DOPE monolayers or glass treated with C-ANO2. These results indicate that the C-ANO2 absorption dipoles were randomly oriented with respect to the polar angle θ, whereas the dil absorption dipoles were ordered. The qualitative observation that $I(\psi)$ was much higher for dil when $\psi = 90°$

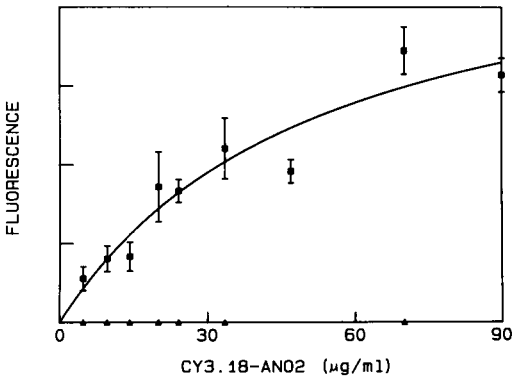

FIGURE 6 C-ANO2 antibodies on supported phospholipid monolayers. Shown is the background-corrected fluorescence for C-ANO2 bound to (■) DSPC/DNP-DOPE and (▲) DSPC supported monolayers as a function of the solution concentration of C-ANO2 with which monolayers were treated.

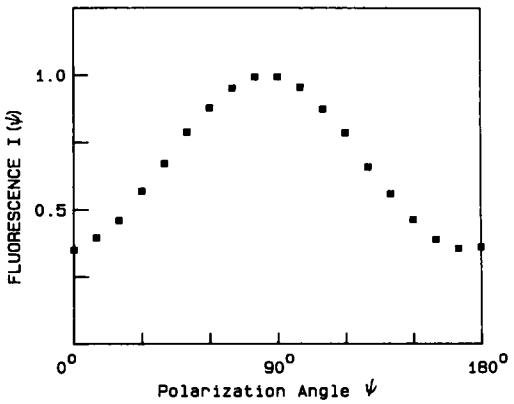

FIGURE 7 Fluorescence-detected absorption dichroism. Shown is the average of four measurements of the fluorescence, I, as a function of the direction of polarization of the totally internally-reflected laser beam, ψ, for dil in DSPC/DNP-DOPE monolayers treated with ANO2 antibodies. The data were normalized as described in the text. The angle ψ is defined in Thompson et al. (1984).

TABLE 2 **Fractional fluorescence changes for dil and C-ANO2 associated with supported monolayers**

Polarization (bleach)	dil/DSPC	dil/DSPC/DNP-DOPE	dil/DSPC/DNP-DOPE and ANO2	DSPC/DNP-DOPE and C-ANO2
A. Circular (no)	0.009 ± 0.003	0.007 ± 0.007	0.016 ± 0.016	0.002 ± 0.001
B. Circular (yes)	0.002 ± 0.001	0.002 ± 0.002	0.008 ± 0.005	0.012 ± 0.005
C. Linear (∥)	0.035 ± 0.003	0.022 ± 0.011	0.034 ± 0.003	0.042 ± 0.012
D. Linear (⊥)	−0.038 ± 0.002	−0.048 ± 0.004	−0.043 ± 0.004	0.007 ± 0.006

Average values and standard errors in the mean were calculated from experimental curves as $[F(\infty) - F(-)]/F(-)$ for *A*, and $[F(\infty) - F(0)]/F(-)$ for *B–D*, where $F(-)$ is the prebleach fluorescence, $F(0)$ is the fluorescence immediately after the bleach pluse, $F(\infty) \approx F(5\text{ min})$ for dil and $F(\infty) \approx F(2\text{ min})$ for C-ANO2.

suggests that the absorption transition dipole moments were approximately parallel to the substrate, consistent with other studies of the orientation of dil or related compounds in model membranes (Axelrod, 1979; Badley et al., 1973).

The values of the constant C obtained from $I(\psi)$ for evanescent illumination were -0.55 ± 0.01 for dil in DSPC monolayers and -0.57 ± 0.01 for dil in DSPC/DNP-DOPE monolayers untreated or treated with unlabeled ANO2 antibodies. These values of C correspond to $s_2 = -0.29 \pm 0.03$ and $s_2 = -0.30 \pm 0.03$ (Fig. 3 *A*). The nonzero magnitude of s_2 argues strongly against the presence of a large number of substrate-absorbed vesicles or other nonplanar structures in which dil could laterally move, giving rise to fluorescence recovery under polarized conditions that was not due to rotational mobility about the normal to the monolayer (e.g., Smith and McConnell, 1981). For stationary dipoles uniformly oriented at a single polar angle $90 - \epsilon$, the measured value of s_2 corresponds to $\epsilon = 22° \pm 2°$ (Eq. 13). For dipoles that are centered at angle ϵ and undergo fast wobbling in a cone of semiangle β, the measured value of s_2 is consistent with a smaller mean value of ϵ; e.g., for $\beta = 20°$, $\epsilon = 20° \pm 2°$, for $\beta = 30°$, $\epsilon = 18° \pm 2°$, and for $\beta = 40°$, $\epsilon = 12° \pm 4°$ (Eq. 14). For the measured value of s_2, the maximum wobble angle, which occurs for $\epsilon = 0°$, is $\beta = 46° \pm 4°$.

Depolarized fluorescence photobleaching recovery

The extent to which postbleach fluorescence changes measured with linearly polarized light might arise from phenomena other than rotational mobility of the lipids or antibodies was assessed using circularly polarized light. In the absence of a bleach pulse, the fluorescence intensity illuminated over a large area was occasionally observed to slowly increase (Table 2 *A*). Similar effects have previously been observed by others and have been attributed to photochemical instabilities (e.g., Smith et al., 1981). The measured fluorescence for this optical configuration also increased slightly after photobleaching, but not at a rate significantly greater than that observed in the absence of bleaching (Table 2 *B*). The fractional postbleach fluorescence changes monitored with linearly polarized light were significant, of comparable magnitudes and positive (or negative) for parallel (or perpendicular) bleaching polarizations (Table 2, *C* and *D*). These results strongly suggest that a significant fraction of the postbleach fluorescence changes measured with linearly polarized light arose from rotational motion of the fluorophore.

Because the most likely source of fluorescence recovery other than rotational mobility is lateral mobility, apparent lateral diffusion coefficients and fractional mobilities were measured with fluorescence pattern photobleaching recovery (Smith and McConnell, 1978) using circularly polarized light and a spatial periodicity of 8 μm (Table 3). The C-ANO2 and dil lateral diffusion coefficients did not significantly differ, which suggests that the antibodies do not undergo significant lateral translation across these solidlike surfaces by detachment of one antigen binding site followed by subsequent attachment at a different position. The measured translational diffusion coefficients and fractional mobilities[2] together with the known functional form for fluorescence recovery due to lateral diffusion in a plane through Gaussian-shaped illumination (Axelrod et al., 1976) imply that the fractional fluorescence recovery due to lateral mobility that would be observed under conditions used for measurement of rotational mobility (25 μm radius and 5 min for dil; 38 μm radius and 2 min for C-ANO2) is small (Table 3).

[2]Without monitoring fluorescence recoveries for much longer times, the experiment cannot distinguish between higher apparent diffusion coefficients with lower fractional mobilities and lower apparent diffusion coefficients with higher fractional mobilities. Results are reported for the maximum diffusion coefficient and minimum fractional mobility.

TABLE 3 **Apparent lateral diffusion coefficients and mobile fractions measured by pattern photobleaching with circularly polarized light**

Sample	D_{lat}	Mobile fraction	Apparent fractional recovery
	10^{-11} cm^2/s		
diI/DSPC	3 ± 2	0.06 ± 0.03	$<2 \times 10^{-4}$
diI/DSPC/DNP-DOPE	20 ± 10	0.12 ± 0.03	$<2 \times 10^{-3}$
diI/DSPC/DNP-DOPE and ANO2	8 ± 2	0.27 ± 0.09	$<2 \times 10^{-3}$
DSPC/DNP-DOPE and C-ANO2	4 ± 2	0.35 ± 0.02	$<2 \times 10^{-4}$

Apparent lateral diffusion coefficients and fractional mobilities and standard errors in the mean were measured using pattern photobleaching with circularly polarized light and a spatial periodicity of 8 μm (see footnote 2). Apparent fractional recoveries were calculated assuming a Gaussian-shaped illumination (Axelrod et al., 1976) and refer to the expected recovery $[F(\infty) - F(0)]/F(-)$ due to lateral mobility under conditions used for rotational mobility (25 μm radius, 5 min for diI; 38 μm radius and 2 min for C-ANO2).

Polarized fluorescence photobleaching recovery of diI

The postbleach fluorescence intensities $F_\parallel(t)$ and $F_\perp(t)$ for diI in supported monolayers increased and decreased for bleaching beam polarization directions parallel and perpendicular to the observation beam polarization, respectively (Fig. 8) and the anisotropies $r(t)$ decayed with time (Fig. 9 *A*) as theoretically predicted (Eqs. 1–9). The anisotropy data could not be well fit with the functional form for a single rotationally diffusing fluorophore (Eq. 4) and were thus fit to the functional form shown in Eq. 7 with $D_1 = 0$ and $R = 2$, 3, and 4. The mean values of the F-statistic that compares the best fits for two components (one mobile and one immobile) and for three components (two mobile and one immobile) were much larger than the critical value of 3.0 (Wright et al., 1988) indicating statistical significance in the increased accuracy of the fit. The mean values of the F-statistic that compares the best fits for three and four components were <3.0. The parameters of the best fits of $r(t)$ to the three-component function are shown in Table 4; additional constants calculated from the best-fit parameters are shown in Table 5. The very slow rotational correlation times (5–100 s) are consistent with previous measurements of diI rotational mobility in solid-phase DSPC multibilayers and liposomes (Smith et al., 1981) and solid-phase DPPC lipid vesicles (Johnson and Garland, 1983).

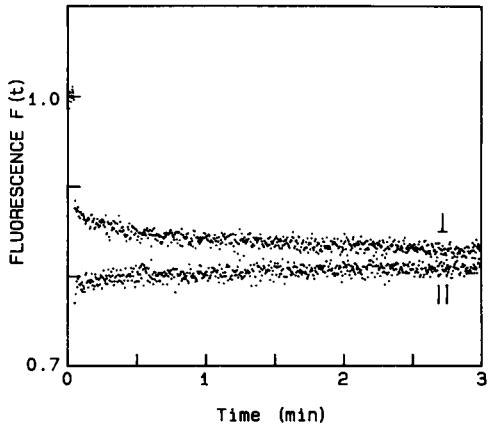

FIGURE 8 PFPR curves $F_\parallel(t)$ and $F_\perp(t)$ for diI in DSPC monolayers. The postbleach fluorescence intensity decays when the bleaching beam is polarized perpendicular to the observation beam and recovers when the bleaching beam is polarized parallel to the observation beam. Shown is the average of three parallel and four perpendicular curves obtained from different positions on a single monolayer.

The total fluorescence change relative to the prebleach fluorescence was 5–10% and the relative magnitudes of each component $(f_i b_i/a)$ were approximately equal so that each component corresponded to only a small postbleach fluorescence change. Thus, the possibilities that the nonmonophasic behavior arose from an unidentified property of the sample or experimental apparatus or overly simple theoretical assumptions leading to the form of Eq. 7 cannot be completely ruled out. The assumptions of uniform (not Gaussian-shaped) illumination and low-aperture microscope optics are only approximately correct, but the assumption that the constant c is of negligible magnitude should be valid (see below). For a single rotationally diffusing fluorophore, the measured difference in the intensity of the bleaching beam when oriented parallel or perpendicular to the monitoring beam (see Materials and Methods) would give rise to an $r(\infty) \approx 0.01$ which is much less than the measured value of $r(\infty) = 0.13$ (Table 5).

The nonmonophasic experimental anisotropies could arise from restricted rotational motion, three or more distinct diI environments, or the presence of small diI oligomers and/or mixed diI/phospholipid aggregates. The second possibility is consistent with the visual observation of inhomogeneities in the spatial distribution of diI and with previous demonstrations of coexistent phases of

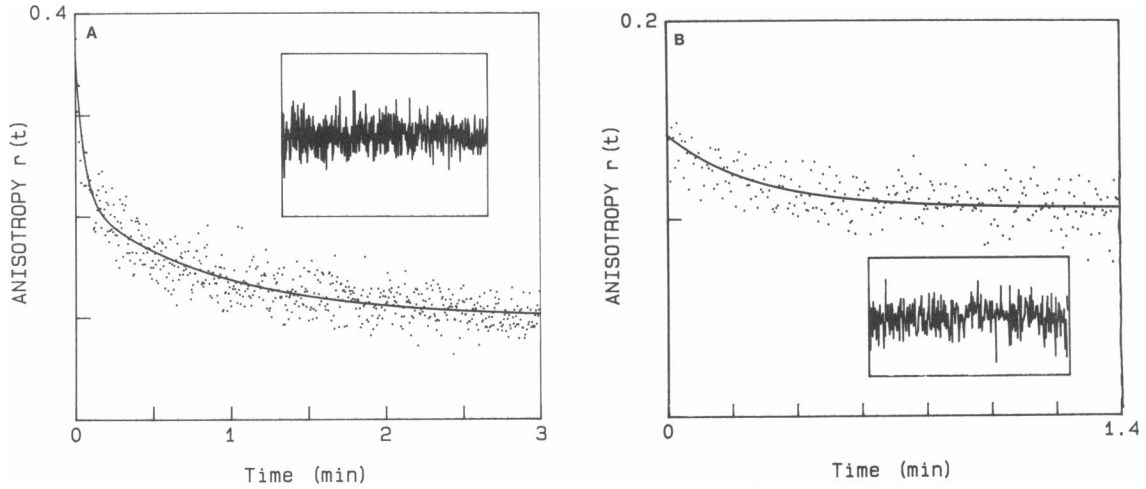

FIGURE 9 PFPR anisotropies $r(t)$. (A) The anisotropy $r(t)$ decays with time for dil in DSPC monolayers. The solid line is the best fit to Eq. 7 with $R = 3$ and $D_1 = 0$; parameter values are $f_1b_1/a = 0.14$, $f_2b_2/a = 0.15$, $f_3b_3/a = 0.17$, $D_2 = 2.7 \times 10^{-3}\ s^{-1}$, and $D_3 = 45 \times 10^{-3}\ s^{-1}$. ($B$) The anisotropy $r(t)$ decays for C-ANO2 on DSPC/DNP-DOPE monolayers. The solid line is the best fit to Eq. 7 with $R = 2$ and $D_1 = 0$; parameter values are $f_1b_1/a = 0.15$, $f_2b_2/a = 0.05$, and $D_2 = 9.4 \times 10^{-3}\ s^{-1}$. Insets show the residuals of the theoretical fits.

different effective viscosities in both liposomes (Wu and McConnell, 1975; Shimshick and McConnell, 1973; Johnson and Garland, 1983) and phospholipid monolayers (Seul et al., 1985; McConnell et al., 1984) of pure and mixed lipid compositions. However, the extent to which dil partitions between fluidlike and solidlike phases may depend on a number of factors (Ethier et al., 1983; Packard and Wolf, 1985). The third possibility agrees with previous reports of the formation of dil aggregates in model membranes (Ethier et al., 1983; Klausner and Wolf, 1980).

None of the measured parameters for the rotational motion of dil in DSPC monolayers and DSPC/DNP-DOPE monolayers untreated and treated with unlabeled ANO2 antibodies were statistically different according to two-tailed t-tests with a 95% confidence limit (Table 4). This result is at first surprising in that the fractional lateral mobility of dil increased with the presence of DNP-DOPE and bound ANO2 (Table 3), suggesting either that the DSPC/DNP-DOPE films are more fluidlike or that a larger fraction of the dil resides in fluidlike regions in DSPC/DNP-DOPE monolayers. However, the multiplicity of possible physical explanations for the measured nonmonophasic anisotropies together with the limitations of the statistical accuracy of the data probably account for the insensitivity of the PFPR data to the presence of DNP-DOPE and bound, unlabeled ANO2.

If the three components reflect distinct dil populations and if the values of b_i, which depend on the orientation and flexibility of the absorption dipole moments of the ith population, are equivalent, then $b_T \approx bi \approx 0.10$ (Table 5). This value together with the measured value of $a = 0.25$ implies that the bleaching parameter $B \approx 0.7$ and wobble angle $\beta \approx 40°$ for $\epsilon = \chi = 0°$ (Fig. 2 A) and that $B \approx 0.8$

TABLE 4 Measured characteristics of dil rotational mobility in supported monolayers

	DSPC	DSPC/DNP-DOPE	DSPC/DNP-DOPE and ANO2
$\Delta F_{\parallel}(0)$	0.32 ± 0.04	0.34 ± 0.03	0.33 ± 0.04
$\Delta F_{\perp}(0)$	0.15 ± 0.03	0.18 ± 0.03	0.15 ± 0.04
f_1b_1/a	0.17 ± 0.04	0.19 ± 0.05	0.19 ± 0.09
f_2b_2/a	0.11 ± 0.01	0.08 ± 0.02	0.09 ± 0.02
f_3b_3/a	0.17 ± 0.04	0.09 ± 0.03	0.11 ± 0.01
$D_2\ (10^{-3}\ s^{-1})$	3.1 ± 0.6	2.1 ± 0.3	2.6 ± 0.4
$D_3\ (10^{-3}\ s^{-1})$	46 ± 9	56 ± 19	71 ± 14
F-statistic	70	31	35

Shown are the average values and standard errors in the mean of the independent parameters measured from PFPR curves for dil in supported phospholipid monolayers.

TABLE 5 **Calculated characteristics of dil rotational mobility in supported monolayers**

	DSPC	DSPC/DNP-DOPE	DSPC/DNP-DOPE and ANO2
a (Eq. 5)	0.24 ± 0.03	0.26 ± 0.02	0.24 ± 0.03
$b_T = \frac{1}{2}[\Delta F_\parallel(0) - \Delta F_\perp(0)]$	0.09 ± 0.03	0.08 ± 0.02	0.09 ± 0.03
$*b_T^c = a\Sigma_{i=1}^{3}\ (f_i b_i/a)$	0.11 ± 0.02	0.09 ± 0.02	0.09 ± 0.02
$*f_1^c = (a/b_T^c)\,(f_1 b_1/a)$	0.37 ± 0.12	0.52 ± 0.19	0.48 ± 0.27
$*f_2^c = (a/b_T^c)\,(f_2 b_2/a)$	0.25 ± 0.05	0.22 ± 0.06	0.24 ± 0.10
$*f_3^c = (a/b_T^c)\,(f_3 b_3/a)$	0.38 ± 0.11	0.26 ± 0.10	0.28 ± 0.08
$\tau_2 = 1/(4D_2)$ (s)	81 ± 16	120 ± 19	96 ± 14
$\tau_3 = 1/(4D_3)$ (s)	5.4 ± 1.1	4.5 ± 1.5	3.5 ± 0.7
$r(0) = 2(b_T/a)/[3 - (b_T/a)]$	0.29 ± 0.10	0.23 ± 0.06	0.29 ± 0.10
$r(\infty) = 2(f_1 b_1/a)/[3 - (f_1 b_1/a)]$	0.12 ± 0.03	0.13 ± 0.04	0.13 ± 0.06

Parameters were calculated according to the equations in the first column and using the measured constants shown in Table 4. *These constants are estimates dependent on the assumption that $b_1 = b_2 = b_3$ (Eq. 9).

and $\beta \approx 30°$ for $\epsilon = \chi = 30°$ (Fig. 2 *B*). For a wobble angle β between 30° and 40°, the measured order parameter, S_2, implies that the average tilt angle ϵ is between 10° and 20° (Eq. 14). For $a = 0.25$, $b = 0.10$, $\epsilon < 30°$ and $\chi < 30°$, the value of c is ~0.001 (calculated as described in Fig. 2) and the assumption that constant c (Eqs. 2 and 6) is of negligible magnitude is valid.

Polarized fluorescence photobleaching recovery of C-ANO2

Measured anisotropies $r(t)$ for C-ANO2 on DSPC/DNP-DOPE monolayers decayed with characteristic times of 10–100 s but to nonzero values at long times (Fig. 9 *B*). Similar to dil, one possible explanation for the measured nonzero anisotropy at long times is that the antibodies do not undergo full rotational diffusion about the monolayer normal. Slow but restricted antibody mobility could arise from lateral motions of the haptenated lipids to which antibodies are bound or from antibody segmental flexibility about two essentially immobile antigen binding sites. Another explanation for the nonzero long-time anisotropies is that the antibodies reside in different environments. Different environments could arise from preexistent or antibody-induced phases including antibody aggregation.

In the simplest case of two environments (mobile and immobile), the anisotropy would have the functional form of Eq. 7 with $R = 2$ and $D_1 = 0$. Experimentally obtained curves $r(t)$ for C-ANO2 on supported monolayers were fit to this functional form to obtain the best values of $f_1 b_1/a, f_2 b_2/a$ and $D_2 = D$ and the values of a and $b_T = (f_1 b_1 + f_2 b_2)$ were calculated from the values of $\Delta F_\parallel(0)$ and $\Delta F_\perp(0)$. For samples treated with low C-ANO2 concentrations (20 μg/ml) for a short time (10 min), the apparent rotational correlation time and fractional mobility were ~70 s and ~0.3, respectively (Table 6). The measured values of a and b_T suggest that the bleaching parameter, B, is ~1.8 and that the semiangle of a cone in which the carbocyanine fluorophores rapidly wobble, β, is ~45° (Fig. 2 *C*).

Antibodies can spontaneously form two-dimensional ordered arrays when specifically bound to supported phospholipid monolayers and bilayers; the array forma-

TABLE 6 **Characteristics of C-ANO2 rotational mobility on supported monolayers**

[C-ANO2] (μg/ml)	20	50	20	20
Time (min)	10	10	1,200	10
Anti-IgG	No	No	No	Yes
Fractional bleach a	0.33 ± 0.05	0.20 ± 0.06	0.29 ± 0.04	0.27 ± 0.04
$f_1 b_1/a$	0.12 ± 0.03	0.15 ± 0.06	0.14 ± 0.04	0.16 ± 0.03
$f_2 b_2/a$	0.045 ± 0.006	0.054 ± 0.010	0.051 ± 0.010	0.010 ± 0.005
Coefficient D (10^{-3} s^{-1})	3.4 ± 0.8	2.7 ± 0.6	4.9 ± 2.4	3.0 ± 2.3
Initial anisotropy $r(0)$*	0.12 ± 0.02	0.14 ± 0.01	0.14 ± 0.04	0.12 ± 0.03
Rotational correlation time (s)*	73 ± 16	92 ± 22	51 ± 25	84 ± 65
Apparent mobile fraction f_2‡	0.27 ± 0.06	0.26 ± 0.10	0.27 ± 0.08	0.06 ± 0.03
Fractional decay/recovery b_T‡	0.05 ± 0.01	0.04 ± 0.03	0.06 ± 0.02	0.04 ± 0.01

Shown at the top are average values and standard errors in the mean of the parameters of C-ANO2 rotational mobility obtained from the best fits of $r(t)$ to Eq. 7 with $R = 2$, $D_1 = 0$ and $D_2 = D$ ($f_i b_i/a$ and D) and from the values of the postbleach fluorescence intensities at time zero and Eq. 5 (a). Shown at the bottom are additional parameters calculated (*) or estimated (‡) as described in Table 5.

tion is more likely to occur at higher antibody surface densities and after longer times (Uzgiris and Kornberg, 1983; Uzgiris, 1985, 1986). Thus, one might expect the rotational mobility of monolayer-bound antibodies to decrease with these factors. However, as shown in Table 6, higher C-AN02 concentrations (50 μg/ml) and longer treatment times (20 h) had no measurable effect on the apparent rotational diffusion coefficient and fractional mobility averaged over all samples.[3] This result indicates either that ordered antibody arrays did not form, which is consistent with the known sensitivity of that phenomenon to environmental factors (e.g., lipid fluidity; Uzgiris, 1985) or that such arrays were present but the monolayer-bound antibodies nonetheless retained some slow rotational or segmental flexibility.

Cross-linking monolayer-bound C-AN02 with unlabeled polyclonal anti-(mouse IgG) antibodies resulted in a decrease in the apparent mobile fraction (Table 6). All of the suggested mechanisms that could give rise to polarization-sensitive postbleach fluorescence changes (full antibody rotation, antibody segmental flexibility, and rotation of lipid domains to which antibodies are bound) are consistent with a decreasing mobile fraction in the presence of a cross-linking antibody: fully mobile antibodies could be immobilized due to an increase in particle size, regional flexibility could be hindered and adjacent phospholipid domains could become aggregated.

The characteristic decay time (~70 s) and long-time nonzero values of $r(t)$ for C-AN02 on supported monolayers are similar to the characteristics observed for diI. Faster recovery times (~4 s) could also be present for monolayer-bound C-AN02, but would not be detectable in the experiments described herein because of the bleach pulse duration (2 s). Thus, the rotational mobility of antibodies specifically bound to model membranes may be as rapid as the lipid rotational mobility. The analogous result has previously been reported for antibody and lipid translational mobility on other model membranes for some conditions (Smith et al., 1979; Wright et al., 1988; Subramaniam et al., 1986; Tamm, 1988).

SUMMARY

The aggregation of antibodies and/or antibody receptors on target cell surfaces or in the region of contact between phagocytotic effector cells and their targets has been suggested as a key factor in the onset of target ingestion (Metzger, 1979; McCloskey and Poo, 1984). The observations that antibodies bound to supported phospholipid monolayers can exhibit inhomogeneous translational diffusion (Wright et al., 1988) and can also form two-dimensional ordered arrays (Uzgiris and Kornberg, 1983) suggests that the monolayer-bound antibodies may experience intermolecular interactions that lead to small aggregate formation. Rotational mobility should be a sensitive indicator of the presence of antibody aggregates.

In this work, polarized fluorescence photobleaching recovery was used to characterize the rotational mobility of fluorescent lipids and fluorescently-labeled antibodies associated with model target cell surfaces. The data confirm that fluorescent lipids in solidlike model membranes undergo very slow rotational mobility on the order of seconds to minutes and indicate that the rotational mobility cannot be described as a simple, monomeric rotational diffusion about the axis normal to the monolayer. Addition of significant amounts of a dinitrophenylated phospholipid followed by anti-dinitrophenyl antibodies had little effect on the lipid probe rotational mobility. The data also indicate that specifically-bound, fluorescently-labeled antibodies are rotationally mobile with a characteristic time approximately equal to that of the fluorescent lipids and therefore provide no evidence for the presence of large antibody oligomers. The results show that, as for fluorescent lipids, the antibody rotational mobility cannot be described as a simple rotational diffusion about the monolayer normal, implying that either bound antibodies are significantly restricted in their rotational mobility or that the bound antibodies reside in more than one environment.

This work contributes to the currently small number of experimental demonstrations of the potential of PFPR as a probe of molecular rotational mobility. Adaptation of PFPR to faster times and the use of signal averaging to increase the statistical accuracy of the data (e.g., Velez and Axelrod, 1988) may reveal more details of antibody rotational mobility on solidlike supported monolayers and may be applicable to antibodies on more fluidlike supported model membranes. The relationship between antibody rotational mobility and cellular recognition of antibody-coated supported monolayers could then be characterized.

APPENDIX A: ORDER PARAMETER FOR WOBBLING ABSORPTION DIPOLES

The laboratory frame is denoted by orthogonal coordinates x, y, and z and polar and azimuthal angles θ and ϕ. A population of fluorophore absorption dipoles is contained in a cone of semiangle β centered at polar angle $\delta = 90° - \epsilon$ and in the $x - z$ plane ($\phi = 0$). An additional frame, denoted by coordinates x', y', z', θ', and ϕ', is defined as a rotation through angle δ about the $y = y'$ axis. The normalized distribution of

[3]The measured values of D were variable from sample to sample. Comparison of carefully matched data suggested that the C-ANO2 rotational correlation times were approximately twofold slower for samples treated with the higher antibody concentration or for longer times.

absorption dipoles in the primed frame is given by

$$N(\theta') = \begin{cases} [2\pi(1 - \cos\beta)]^{-1} & 0 < \theta' < \beta \text{ and } 0 < \phi' < 2\pi \\ 0 & \text{otherwise.} \end{cases} \quad \text{(A1)}$$

Then,

$$s_2 = \tfrac{1}{2}[3\langle\cos^2\theta\rangle - 1] \quad \text{(A2)}$$

$$\langle\cos^2\theta\rangle = [2\pi(1 - \cos\beta)]^{-1} \int_0^{2\pi}\int_0^{\beta} \cos^2\theta \sin\theta' \, d\theta' \, d\phi' \quad \text{(A3)}$$

$$\cos\theta = z'\cos\delta - x'\sin\delta \quad \text{(A4)}$$

$$z' = \cos\theta', \quad x' = \sin\theta'\cos\phi'. \quad \text{(A5)}$$

Substituting Eq. A5 into Eqs. A4, A3, and A2 yields Eq. 14.

We thank Daniel Axelrod of the University of Michigan for numerous helpful conversations, Alan Waggoner and Ratan Majumdar of Carnegie-Mellon University for the carbocyanine dye CY3.18 with which ANO2 antibodies were labeled, Harden McConnell of Stanford University for ANO2 hybridoma cells, and Arthur Palmer of the Scripps Institute and Mary Lee Pisarchick and Claudia Poglitsch of the University of North Carolina for their contributions to various biochemical and optical aspects of this work.

Support was provided by National Institutes of Health Grant GM-37145, National Science Foundation Presidential Young Investigator Award DCB-8552986, and a University of North Carolina Junior Faculty Development Award.

Received for publication 7 November 1989 and in final form 29 March 1990.

REFERENCES

Anglister, J., T. Frey, and H. M. McConnell. 1984. Magnetic resonance of a monoclonal anti-spin label antibody. *Biochemistry.* 23:1138–1142.

Axelrod, D. 1977. Cell surface heating during fluorescence photobleaching recovery experiments. *Biophys. J. 18:129–131.*

Axelrod, D. 1979. Carbocyanine dye orientation in red cell membrane studied by microscopic fluorescence polarization. *Biophys. J.* 26:557–574.

Axelrod, D., D. E. Koppel, J. Schlessinger, E. Elson, and W. W. Webb. 1976. Mobility measurement by analysis of fluorescence photobleaching recovery kinetics. *Biophys. J.* 16:1055–1069.

Badley, R. A., W. G. Martin, and H. Schneider. 1973. Dynamic behavior of fluorescent probes in lipid bilayer model membranes. *Biochemistry.* 12:268–275.

Balakrishnan, K. F., F. J. Hsu, D. G. Hafeman, and H. M. McConnell. 1982. Monoclonal antibodies to a nitroxide lipid hapten. *Biochim. Biophys. Acta.* 721:30–38.

Burghardt, T. P., and N. L. Thompson. 1984. Effect of planar dielectric interfaces on fluorescence emission and detection. *Biophys. J.* 46:729–737.

Chen, R. F., and C. H. Scott. 1985. Atlas of fluorescence spectra and lifetimes of dyes attached to protein. *Anal. Lett.* 18:393–421.

Dale, R. E. 1985. Interpretation of fluorescence photobleaching recovery experiments on oriented cell membranes. *FEBS (Fed. Eur. Biophys. Soc.) Lett.*, 192:255–258.

Dale, R. E. 1987. Depolarized fluorescence photobleaching recovery. *Eur. Biophys. J.* 14:179–193.

Ethier, M. F., D. E. Wolf, and D. L. Melchior. 1983. Calorimetric investigation of the phase partitioning of the fluorescent carbocyanine probes in phosphatidylcholine bilayers. *Biochemistry.* 22:1178–1182.

Hafeman, D. G., V. von Tscharner, and H. M. McConnell. 1981. Specific antibody-dependent interactions between macrophages and lipid haptens in planar lipid monolayers. *Proc. Natl. Acad. Sci. USA.* 78:4552–4556.

Johnson, P., and P. B. Garland. 1983. Carbocyanine dyes used as fluorescent triplet probes for measuring slow rotational diffusion of lipids in membranes. *FEBS (Fed. Eur. Biophys. Soc.) Lett.*, 153:391–394.

Kimura, K., M. Nakanishi, M. Ueda, J. Ueno, H. Nariuchi, S. Furukawa, and T. Yasuda. 1986. The effect of immunoglobulin G1 structure on macrophage binding to supported planar lipid monolayers. *Immunology.* 59:235–238.

Klausner, R. D., and D. E. Wolf. 1980. Selectivity of fluorescent lipid analogues for lipid domains. *Biochemistry.* 19:6199–6203.

Leach, S. J. 1969. Physical Principles and Techniques of Protein Chemistry. Academic Press, Inc., New York. 184–185.

Leahy, D. J., G. S. Rule, M. M. Whittaker, and H. M. McConnell. 1986. Sequences of 12 monoclonal anti-dinitrophenyl spin-label antibodies for NMR studies. *Proc. Natl. Acad. Sci. USA.* 85:3661–3665.

McCloskey, M., and M. M. Poo. 1984. Protein diffusion in cell membranes: some biological implications. *Int. Rev. Cytol.* 87:19–81.

McConnell, H. M., L. K. Tamm, and R. M. Weis. 1984. Periodic structures in lipid monolayer phase transitions. *Proc. Natl. Acad. Sci. USA.* 81:3249–3253.

McConnell, H. M., T. H. Watts, R. M. Weis, and A. A. Brian. 1986. Supported planar membranes in studies of cell-cell recognition in the immune system. *Biochim. Biophys. Acta.* 864:95–106.

Metzger, H. 1979. Early molecular events in antigen-antibody cell activation. *Ann. Rev. Pharmacol. Toxicol.* 19:427–445.

Mishell, B. B., and S. M. Shiigi. 1980. *Selected Methods in Cellular Immunology.* W. H. Freeman & Co., San Francisco. 295.

Packard, B. S., and D. E. Wolf. 1985. Fluorescence lifetimes of carbocyanine lipid analogues in phospholipid bilayers. *Biochemistry.* 24:5176–5181.

Palmer, A. G., and N. L. Thompson. 1989. High-order fluorescence fluctuation analysis of model protein clusters. *Proc. Natl. Acad. Sci. USA.* 86:6148–6152.

Peterson, G. L. 1979. Review of the Folin phenol protein quantitation method of Lowry, Rosebrough, Farr and Randall. *Anal. Biochem.* 100:201–220.

Poglitsch, C. L., and N. L. Thompson. 1990. Interaction of antibodies with Fc receptors in substrate-supported planar membranes measured by total internal reflection fluorescence microscopy. *Biochemistry.* 29:248–254.

Scalettar, B. A., P. R. Selvin, D. Axelrod, J. E. Hearst, and M. P. Klein. 1988. A fluorescence photobleaching study of the microsecond reorientational motions of DNA. *Biophys. J.* 53:215–226.

Scalettar, B. A., P. R. Selvin, D. Axelrod, M. P. Klein, and J. E. Hearst. 1990. A polarized photobleaching study of DNA reorientation in agarose gels. *Biochemistry.* 29:4790–4798.

Seul, M., S. Subramaniam, and H.M. McConnell. 1985. Mono- and bilayers of phospholipids at interfaces: interlayer coupling and phase stability. *J. Phys. Chem.* 89:3592–3595.

Shimshick, E. J., and H. M. McConnell. 1973. Lateral phase separation in phospholipid membranes. *Biochemistry.* 12:2351–2360.

Smith, B. A., and H. M. McConnell. 1978. Determination of molecular motion in membranes using periodic pattern photobleaching. *Proc. Natl. Acad. Sci. USA.* 75:2759–2763.

Smith, L. M., and H. M. McConnell. 1981. Pattern photobleaching of fluorescent phospholipid vesicles using polarized laser light. *Biophys. J.* 33:139–146.

Smith, L. M., J. W. Parce, B. A. Smith, and H. M. McConnell. 1979. Antibodies bound to lipid haptens in model membranes diffuse as rapidly as the lipids themselves. *Proc. Natl. Acad. Sci. USA.* 76:4177–4179.

Smith, L. M., R. M. Weis, and H. M. McConnell. 1981. Measurement of rotational motion in membranes using fluorescence recovery after photobleaching. *Biophys. J.* 36:73–91.

Subramaniam, S., M. Seul, and H. M. McConnell. 1986. Lateral diffusion of specific antibodies bound to lipid monolayers on alkylated substrates. *Proc. Natl. Acad. Sci. USA.* 83:1169–1173.

Tamm, L. K. 1988. Lateral diffusion and fluorescence microscope studies of a monoclonal antibody specifically bound to supported phospholipid bilayers. *Biochemistry.* 27:1450–1457.

Thompson, N. L., and A. G. Palmer. 1988. Model cell membranes on planar substrates. *Comments Mol. Cell. Biophys.* 5:39–56.

Thompson, N. L., H. M. McConnell, and T. P. Burghardt. 1984. Order in supported phospholipid monolayers detected by the dichroism of fluorescence excited with polarized evanescent illumination. *Biophys. J.* 46:739–747.

Thompson, N. L., A. G. Palmer, L. L. Wright, and P. E. Scarborough. 1988. Fluorescence techniques for supported planar model membranes. *Comments Mol. Cell. Biophys.* 5:109–131.

Uzgiris, E. E. 1985. Antibody crystallization on phospholipid films: dynamics and the effects of antibody conformation. *J. Cell. Biochem.* 29:239–251.

Uzgiris, E. E. 1986. Supported phospholipid bilayers for two-dimensional protein crystallization. *Biochem. Biophys. Res. Commun.* 134:819–826.

Uzgiris, E. E., and R. D. Kornberg. 1983. Two-dimensional crystallization technique for imaging macromolecules, with application to antigen-antibody-complement complexes. *Nature (Lond.).* 301:125–129.

Velez, M., and D. Axelrod. 1988. Polarized fluorescence photobleaching recovery for measuring rotational diffusion in solutions and membranes. *Biophys. J.* 53:575–591.

von Tscharner, V., and H. M. McConnell. 1981. Physical properties of lipid monolayers on alkylated planar glass surfaces. *Biophys. J.* 36:421–427.

Wagner, M., L. Ernst, R. Majumdar, S. Majumdar, J. Chao, and A. Waggoner. 1990. Applications of new cyanine labeling reagents in flow cytometry. 14th International Meeting of the Society for Analytical Cytology, Asheville, NC. Abstract No. 459.

Wegener, W. A. 1984. Fluorescence recovery spectroscopy as a probe of slow rotational motions. *Biophys. J.* 46:795–803.

Wegener, W. A., and R. Rigler. 1984. Separation of translational and rotational contributions in solution studies using fluorescence photobleaching recorvery. *Biophys. J.* 46:787–793.

Wright, L. L., A. G. Palmer, and N. L. Thompson. 1988. Inhomogeneous translational diffusion of monoclonal antibodies on phospholipid Langmuir-Blodgett films. *Biophys. J.* 54:463–470.

Wu, S. H., and H. M. McConnell. 1975. Phase separations in phospholipid membranes. *Biochemistry.* 14:847–854.

Yguerabide, J., and L. Stryer. 1971. Fluorescence spectroscopy of an oriented model membrane. *Proc. Natl. Acad. Sci. USA.* 68:1217–1221.